Ground-state electronic structure and electronic excitations of small iron clusters

1992 J. Phys.: Condens. Matter 4 6417

(http://iopscience.iop.org/0953-8984/4/30/008)

J. Phys.: Condens. Matter 4 (1992) 6417–6428. Printed in the UK

Ground-state electronic structure and electronic excitations of small iron clusters

L I Kurkina and O V Farberovich

Faculty of Physics, Voronezh State University, University Square 1, 394693 Voronezh, Russia

Received 17 November 1991, in final form 9 April 1992

Abstract. Using the local spin-density approximation and the 'atom in jellium' model, the size dependences of the electronic structure, ionization potential and photoabsorption cross section of iron clusters containing up to 130 atoms are obtained. It is shown that the filling of localized atomic d states of iron clusters changes non-monotonically depending on the position of the atom in relation to the cluster surface as well as on the cluster size. The non-monotonic change of the electronic structure with increase of iron cluster size results in the non-monotonic size dependence of the physical properties of the iron cluster presented here.

1. Introduction

Small metal clusters (SMC) show anomalous physical and chemical properties in comparison with the behaviour of the corresponding bulk solids and free atoms. In recent years, the unique characteristics of SMC have attracted great attention. Size-selective chemical and physical properties of microclusters are of special interest. The fact is that SMC are excellent catalysts, which are used effectively in tehnological processes including heterogeneous catalysis, and it is well known that the activity and selectivity of such catalysts depend on the cluster size. Furthermore, SMC are interesting as research models for problems in solid-state physics and chemistry. For these reasons, size properties of SMC have been studied intensively by both experiment and theory. Lately, methods to produce clusters of controlled size have been developed [1, 2], and the size dependence of some characteristics of microclusters have been measured (for example, magnetic moment [3], chemisorption reactivity [4], ionization potential [5, 6]).

Theoretical investigations of the physical properties of clusters have been carried out actively, too. A variety of theoretical models have been proposed for calculations of cluster electronic structure. However, most precise models (such as the self-consistent-field $X\alpha$ scattered-wave method or some other methods) permit one to obtain the electronic structure for clusters with a low number of atoms. For large atomic aggregations, these methods cannot be applied successfully, and simpler models are employed in this case. Thus, for the study of electronic properties of sp-bonded metal clusters, a jellium model is used, and it gives an excellent description of various experimentally observed data [7–17]. But models such as the jellium approximation are unsuitable for investigations of metal clusters containing atoms with d- or f-localized shells.

0953-8984/92/306417+12$04.50

In this paper we have made an attempt to study the size dependence of the electronic structure, ionization potential and photoabsorption cross section for spherical iron clusters within the framework of the 'atom in jellium' model. Recently we have applied this model for calculations of some magnetic properties of small iron clusters [18].

2. Electronic structure

2.1. Model and method

Each atom of a cluster is mimicked by the same atom embedded in the centre of a jellium sphere with radius R, which is determined according to the position of the real atom in relation to the cluster surface: R defines the short cut between the atom and the cluster surface.

The electronic structure of an atom embedded in a jellium sphere is obtained using self-consistent Kohn–Sham equations (in atomic Rydberg units)

$$[-\nabla^2 + V^s(r)]\psi_{nls}(r) = E_{nls}\psi_{nls}(r) \tag{1}$$

$$V^s(r) = -\frac{2Z}{r} + 2\int \frac{n^-(r') - n^+(r')}{|r - r'|}\,dr' + V^s_{xc}(r) \tag{2}$$

$$n^-(r) = \sum_{nls} f_{nls}|\psi_{nls}(r)|^2 \tag{3}$$

with the Vosko form [19] of the local spin-polarized exchange–correlation potential $V^s_{xc}(r)$. Here the spin s is $\uparrow, \downarrow$; Z is the central nuclear charge; and f_{nls} is the electronic state occupation number. The rigid positive charge distribution of the jellium background is given by

$$n^+(r) = n_0^+\theta(R - r)\theta(r - r_c) \tag{4}$$

where $\theta(x)$ is the unit step function, R and r_c being, respectively, the outer and inner radii of the positive background sphere; n_0^+ is the same as the mean valence electron density of the corresponding bulk metal:

$$n_0^+ = 3N/4\pi(R^3 - r_c^3) \tag{5}$$

$$R = (N/N_a + 1)^{1/3}r_c \tag{6}$$

where r_c is the Wigner–Seitz radius, N is the number of electrons in the jellium sphere, and N_a is the number of valence electrons in an atom of the cluster. For Fe we have employed $r_c = 2.67$ au and $N_a = 2$.

The Hermann–Skillman mesh [20] for a free Fe atom was used for the numerical integration of the Kohn–Sham equation for the 'Fe atom in jellium sphere system'.

The abstract shape of the self-consistent potential $V(r)$ (equation (2)) for an Fe atom embedded in a jellium sphere is presented in figure 1.

Electronic ground-state configurations of jellium clusters containing the central Fe atom were determined in the following way. The rules for the energy level occupation separately in jellium (in a spherical potential well) and in a free atom are well known.

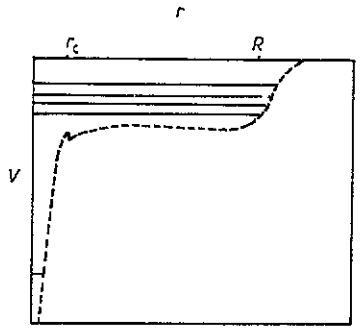

Figure 1. The self-consistent potential of the jellium sphere containing the central Fe atom (the radial distribution).

Clearly, insertion of an atom in the jellium sphere centre does not change the atom and jellium field symmetry, and, consequently, the symmetry of their electron states is not changed either. One can suppose, therefore, that the number of electron states with the same symmetry in the jellium sphere with the central atom is equal to the sum of such symmetry states of the jellium and the atom. The sequence of energy levels of an 'atom in jellium' is obtained by solving the spin-polarized self-consistent equations (1)–(3) for the different angular l and principal n quantum numbers. The occupation numbers of the energy levels, with the exception of upper levels, are in accordance with the Pauli principle. The highest levels can be filled partially. We computed, therefore, the total energy of jellium spheres with the Fe atom in the centre for various occupation numbers of the upper levels. The electron configuration with the lowest total energy has been chosen as the ground state.

For the calculation of the total energy we employed the expression:

$$E_{tot} = T + E_{xc} + E_{ee} + E_{ne} + E_{be}. \tag{7}$$

Here

$$T = \sum_{j}^{occ} E_j - \int n_{out}^{-}(r) V^{in}(r)\, dr \tag{8}$$

is the kinetic part of the total energy (here, the sum is over all occupied states; E_j are the one-electron eigenvalues);

$$E_{xc} = \int \mathcal{E}_{xc}^{out}(r) n_{out}^{-}(r)\, dr \tag{9}$$

is the exchange–correlation contribution to the total energy for which the local spin-density approximation is used; $\mathcal{E}_{xc}$ is the exchange–correlation energy density of a homogeneous electron gas of density n^- (for $\mathcal{E}_{xc}$ we applied the spin-polarized parametrization by Vosko *et al* [19]);

$$E_{ee} = \int\int \frac{n_{out}^{-}(r) n_{out}^{-}(r')}{|r - r'|}\, dr\, dr' \tag{10}$$

is the energy of a Coulomb interaction among electrons;

$$E_{ne} = -2Z \int \frac{n_{out}^{-}(r)}{r}\, dr \tag{11}$$

is the energy of the interaction between the electron system and the central atom nucleus; and

$$E_{be} = -2 \int \int \frac{n^+(r) n^-_{out}(r')}{|r - r'|} \, dr \, dr' \tag{12}$$

is the energy of the electron system and jellium positive background interaction.

The effective potential $V(r)$ is given by

$$V^{in}(r) = V^{in}_{xc}(r) + 2 \int \frac{n^-_{in}(r') - n^+(r')}{|r - r'|} \, dr' - \frac{2Z}{r} \tag{13}$$

where $n^-(r)$ is defined by (3) and $n^+(r)$ is found from (4)–(6).

In these expressions 'in' and 'out' mark, respectively, input and output data of the last iteration of self-consistency.

Taking into account (8)–(13), the expression for the total energy (7) can be rewritten as

$$E_{tot} = \sum_j^{occ} E_j + \int n^-_{out}(r) \left(\mathcal{E}^{out}_{xc}(r) - V^{in}_{xc}(r) + \int \frac{n^-_{out}(r') - 2n^-_{in}(r')}{|r - r'|} \, dr' \right) dr. \tag{14}$$

2.2. Results

Our calculations by the above scheme showed that the five lowest energy levels of the Fe atom embedded in jellium spheres with various radii are identical to those of an iron core, and the rest of them are similar to the energy spectrum of a spherical potential well. This order is broken by the d state in the upper part of the occupied energy region. (In this paper the quantity $n = n_n + 1$ has been considered as a principal quantum number; n_n is the number of nodes of the wavefunction corresponding to the energy level.)

We have calculated the electronic structure of the jellium sphere with the iron atom embedded in the centre as a function of the jellium sphere size. It was found that the electronic structure of such a system alters periodically with increase of the jellium sphere radius (or of the number of electrons in the jellium, N, according to (6)). Each period starts when the new empty d level appears and is completed by its full occupation (see table 1). Boundaries of the periods are systems with $N = 10$, 60, 188, 430, etc. In each period the filling of the d level is an uneven process: at the beginning the number of electrons in this level increases sharply up to the configuration d^5, then changes much more slowly to d^{10} (see figure 2). Obviously, this effect is caused by the exchange interaction, which promotes the filling of the d level up to the configuration d^5 and prevents it from d^5 to d^{10}.

The calculations showed that, as the next d level is filled by electrons, the previous d state extends. As an example of this phenomenon, the change of 1d- and 2d-squared wavefunctions of the 'Fe atom in jellium' system during filling of the 2d shell is presented in figure 3. As can be seen in the figure, the 1d electron density has a 'double-hill' shape: the first 'hill' is within the atomic Wigner–Seitz sphere, the other is in the jellium region. At the beginning of the period the great part of the

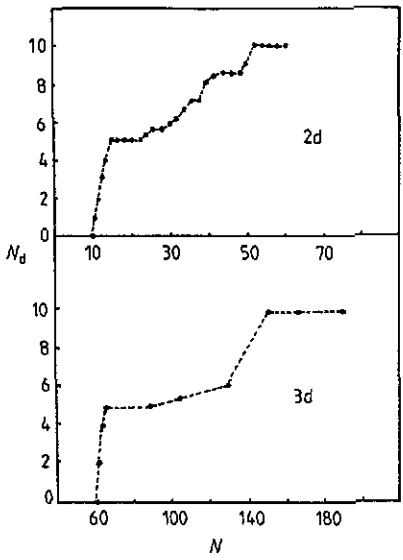

Figure 2. The occupation of 2d and 3d shells of the 'Fe atom in jellium sphere' system as a function of the number of electrons in jellium.

Table 1. The electron configurations of the Fe atom embedded in jellium spheres containing from 10 to 60 electrons.

N	Majority spin	Minority spin
	$1s^1\,2s^1\,1p^3\,3s^1\,2p^3\,4s^1\,3p^3\,1d^5\ldots$	$1s^1\,2s^1\,1p^3\,3s^1\,2p^3\,4s^1\,3p^3\,1d^5\ldots$
10	$\ldots 2d^0$	$\ldots 2d^0$
12	$\ldots 2d^2$	$\ldots 2d^0$
16	$\ldots 2d^5 5s^1$	$\ldots 2d^0 5s^0$
32	$\ldots 2d^5 5s^1 1f^7$	$\ldots 5s^1 1f^7 2d^1$
50	$\ldots 5s^1 1f^7 4p^3 2d^5 1g^9$	$\ldots 5s^1 1f^7 4p^3 2d^4 1g^0$
54	$\ldots 5s^1 1f^7 4p^3 2d^5 1g^9$	$\ldots 5s^1 1f^7 4p^3 2d^5 1g^3$
	$\ldots 5s^1 1f^7 4p^3 2d^5 1g^9\ldots$	$\ldots 5s^1 1f^7 4p^3 2d^5 1g^9\ldots$
60	$\ldots 3d^0$	$\ldots 3d^0$

1d electron density concentrates in the first 'hill'. During the filling of the 2d shell, the 1d electron density redistributes between the two 'hills', and towards the end of the period most of it transfers to the jellium region. The 2d state, in turn, extends during the filling of the 3d level. And so on. So, the most localized of the d states corresponds to the highest occupied d level. However, this state is less localized than the d shell of a free Fe atom, and the extent of it increases with the jellium sphere radius.

Thus, the interaction between d electrons of the Fe atom and s valence electrons of the cluster has led to the periodic occupation of the localized d state of the 'Fe atom in jellium' system with increase of the jellium sphere radius. Within the framework of our model, this effect corresponds to the non-monotonic change of the occupation of localized d states on moving from the surface to the centre of the cluster.

Note that $X\alpha$ scattered-wave calculations [21] of the charge distribution in Fe_{15}

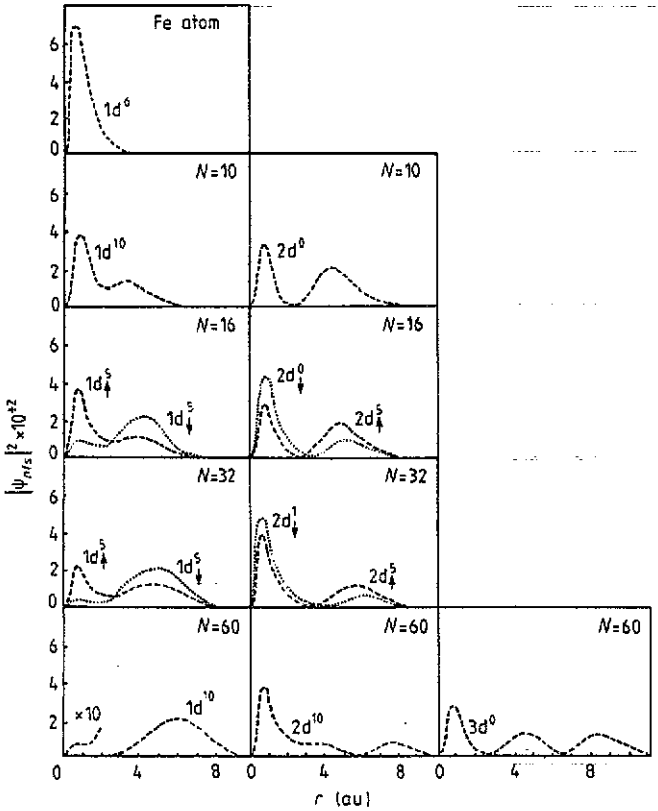

Figure 3. The change of 1d- and 2d-squared wavefunctions of the 'Fe atom in jellium sphere' system during the filling of the 2d shell.

have shown a different number of d electrons in the central and peripheral atoms of the Fe cluster too.

3. Ionization potentials

Recently the study of ionization potentials (IP) of SMC has become of considerable interest. It has been shown [4–6] that the IP of iron atomic aggregations decrease non-monotonically towards the bulk IP, displaying some oscillations. A strong correlation between the chemisorption reactivity of free iron clusters and their ionization thresholds has been shown [4].

In this paper we report the results of our calculations of IP for Fe clusters containing up to 20 atoms. The IP of these atomic systems were experimentally obtained by Rohlfing *et al* [4–6].

In the calculations we simulate atoms of an Fe cluster by Fe atoms embedded in the centre of jellium spheres of various sizes. The jellium sphere radius R is defined by the short cut between the atom and the cluster surface.

The IP of an 'atom in jellium' was obtained using a ground-state theory (the local spin-density approximation) by self-consistent calculation (according to (14)) and subtraction of total energies of the neutral and ionic ground states.

It was found that ionization thresholds of atoms of the Fe cluster are different and depend on the positions of the atoms in relation to the cluster surface. The lowest atomic ionization threshold has been chosen as the IP of the Fe cluster.

The IP of Fe clusters with BCC and FCC structures (cluster atoms are placed around the central atom like BCC or FCC coordination spheres of bulk iron) have been calculated. It was found that the IP of iron clusters containing up to 20 atoms are determined by the IP of its central atoms (that is the IP of the cluster coincides with that of an Fe atom embedded in the centre of the jellium sphere with the radius of this cluster), and do not depend on the cluster geometric structure.

Our model calculations give the size dependence of IP, which is in good qualitative agreement with the known experimental data (figure 4). The IP dependence on the cluster size is non-monotonic, and the ionization thresholds of all clusters considered here are larger than the work function of bulk iron (4.5–4.8 eV). But our results predict a much larger amplitude of IP oscillations than do the experiments. The oscillations on the calculated IP curve arise from the shell character of the model and the non-monotonic occupation of localized d states.

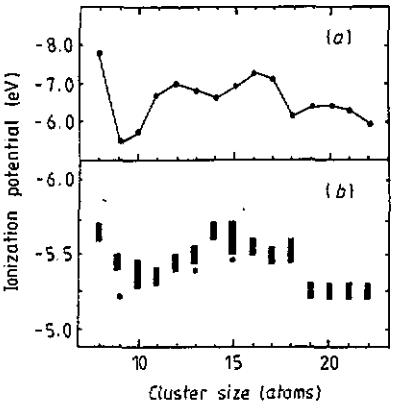

Figure 4. The size dependence of ionization potentials of iron clusters: (*a*) calculations of present work; (*b*) *ab initio* calculations [22–24] (circles) and experiment [27] (rectangles).

For comparison, we cite (see figure 4) the IP for Fe_9 (with assumed BCC geometry), Fe_{13} (FCC) and Fe_{15} (BCC) clusters calculated in [22–24] by the transition-state procedure of Slater within the local spin-density functional theory with a Gaussian orbitals basis. As one can see, the more sophisticated method yields better quantitative agreement with the experimental data than does our method. Note, however, that calculations of electronic properties of transition-metal clusters by the most precise *ab initio* methods have been made for a fairly small number of specific cluster sizes. So, it is difficult to determine the size dependence of IP of Fe clusters on the basis of these results.

Among a variety of calculations of IP using simple models (e.g. [25–27]) we mention the remarkably correct description of the experimental dependence that has been obtained in [25] within a simple tight-binding theory. This theory uses input parameters that yield correctly some bulk iron properties (magnetic moment, work function, compressibility, etc.). In contrast to our conclusion, in [25] it is shown that the IP is dependent on the assumed Fe cluster geometry. These calculations predict different dependences of IP on cluster size for BCC- and FCC-like structures, giving the best agreement with experiment for BCC-like iron clusters.

4. Photoabsorption spectra

It is known that in photoabsorption spectra of atomic 3d metals the strong asymmetric peak near the energy of the 3p excitation is dominant (in the present section the usual atomic classification is employed for designation of free Fe atom states and core shells of an Fe atom embedded in jellium spheres). This peak is interpreted as a giant autoionization resonance [28, 29] and is caused by the existence of unoccupied 3d states and by the large overlap (hence, the strong interaction) between localized 3p and 3d wavefunctions, which results in interference between the discrete $3p \rightarrow 3d$ excitations and the $3d \rightarrow \epsilon l$ ionization channels.

In this section of the paper the change of the giant resonance shape from an Fe atom to iron clusters and bulk metal is studied.

4.1. Model and method

The calculations of the dipole photoabsorption cross section

$$\sigma(w) = \frac{16\pi^2 w|e|}{3c}\operatorname{Im}\sum_s \int_0^\infty \delta n^s(r,w) r^3 \,\mathrm{d}r$$

for a free atom and SMC of iron were carried out within the time-dependent local spin-density approximation [30, 31] using the self-consistent solution of the set of equations:

$$\begin{aligned}
\delta n^s(r,w) &= \int \chi_0^s(r,r',w)\delta V^s(r',w)\,\mathrm{d}r' \\
\delta V^s(r,w) &= V_{\mathrm{ext}}(r,w) + V_{\mathrm{ind}}^s(r,w) \\
V_{\mathrm{ind}}^s(r,w) &= 2\sum_{s'}\int \frac{\delta n^{s'}(r',w)}{|r-r'|}\,\mathrm{d}r' + \sum_{s'}\frac{\partial V_{\mathrm{xc}}^s(r)}{\partial n^{s'}(r)}\delta n^{s'}(r,w). \qquad (15)
\end{aligned}$$

Here $V_{\mathrm{ext}}(r,w)$ and $V_{\mathrm{ind}}(r,w)$ are, respectively, an external field of frequency w and an induced field; $\delta n^s(r,w)$ is the change in the charge density; $\chi_0^s(r,r',w)$ is the susceptibility function in the independent-particle approximation:

$$\begin{aligned}
\chi_0^s(r,r',w) = &\sum_i^{\mathrm{occ}} \psi_{is}(r)\psi_{is}^*(r')G(r,r';E_{is}+w) \\
&+ \sum_i^{\mathrm{occ}} \psi_{is}^*(r)\psi_{is}(r')G^+(r,r';E_{is}-w) \qquad (16)
\end{aligned}$$

where $G(r,r',w)$ is the Green function. Energy levels E_{is} and wavefunctions ψ_{is} of the ground state are obtained as the solution of the Kohn–Sham equations (1)–(3).

In calculations of the iron cluster photoabsorption, we modelled every cluster atom by an Fe atom embedded in the jellium sphere with radius equal to the distance between the atom and the cluster surface. The difference between photoabsorption cross sections of the jellium sphere with the Fe atom in the centre and the same jellium sphere without the inner atom was considered as the photoabsorption of the

single atom, which is 'dressed' in the cluster s–d interaction. The total photoabsorption spectrum of the cluster is obtained as the sum of cross sections of these cluster 'quasi-atoms'.

Thus, we reduced the problem of photoabsorption for the Fe cluster to the spherically symmetric one for the Fe atom embedded in jellium spheres. For spherically symmetric systems, the Green function in (16) has a simple decomposition,

$$G(\boldsymbol{r},\boldsymbol{r}',E)=\sum_{lm}Y_{lm}(\hat{\boldsymbol{r}})G_l(r,r',E)Y^*_{lm}(\hat{\boldsymbol{r}}')$$

where $G_l(r,r',E)$ can be expressed as

$$G_l(r,r',E)=\mathcal{R}_l(r_<,E)\mathcal{N}_l(r_>,E)/r^2W_l(E).$$

$Y_{lm}(\hat{\boldsymbol{r}})$ is a spherical harmonic; $r_<$ and $r_>$ are the lesser and greater of r and r'; $r\mathcal{R}_l(r,E)$ and $r\mathcal{N}_l(r,E)$ are, respectively, regular and irregular solutions, at the origin, of the radial Kohn–Sham equation with the potential (2) and energy E; and $W_l(E)$ is a Wronskian of functions $\mathcal{R}_l$ and $\mathcal{N}_l$.

We obtained $\mathcal{R}_l$ and $\mathcal{N}_l$ by integration of the radial Kohn–Sham equation, using the asymptotic behaviour of these functions at the origin and infinity. As is generally known, the regular solution $\mathcal{R}_l$ behaves asymptotically for $r\rightarrow 0$ as r^{l+1}. When $r\rightarrow\infty$, the irregular solution $\mathcal{N}_l$ must be an outgoing wave for positive energies, and it is exponentially decreasing for negative energies.

So, the well known decomposition

$$r\mathcal{R}_l(r,E)=r^{l+1}\sum_{\nu=0}\beta_\nu r^\nu$$

was used for $\mathcal{R}_l$ at the origin (here factors β_ν can be determined by substituting the decomposition for $\mathcal{R}_l$ into the radial Kohn–Sham equation).

At large radii, the Wentzel–Kramers–Brillouin (WKB) approximation [32] was employed but only for wavefunctions corresponding to the core levels of the central atom. The WKB region for the rest of the levels of the 'Fe atom in jellium' system is beyond the Hermann–Skillman mesh. We applied the phase function method [33] in this case.

4.2. Results

We considered spherical Fe clusters with a BCC geometric structure (cluster atoms are around the central atom like coordination spheres of a BCC structure with $a=2.87$ Å).

The calculated photoabsorption spectra of a free Fe atom and of spherical iron clusters containing from 9 to 127 atoms, and the $M_{2,3}$ absorption spectrum of bulk iron in the energy range 50–60 eV are shown in figure 5.

As can be seen in figure 5(*a*), the theoretical photoabsorption cross section for atomic Fe will correctly reproduce the shape of the experimentally observed spectrum [28] if the calculated curve is moved as a whole to the right by 2 eV. The necessity to move the theoretical results along the energy scale is bound up with the use of the local density approximation, which gives not quite accurate energy eigenvalues and self-consistent potential of the ground state [34]. Since the photoabsorption spectra

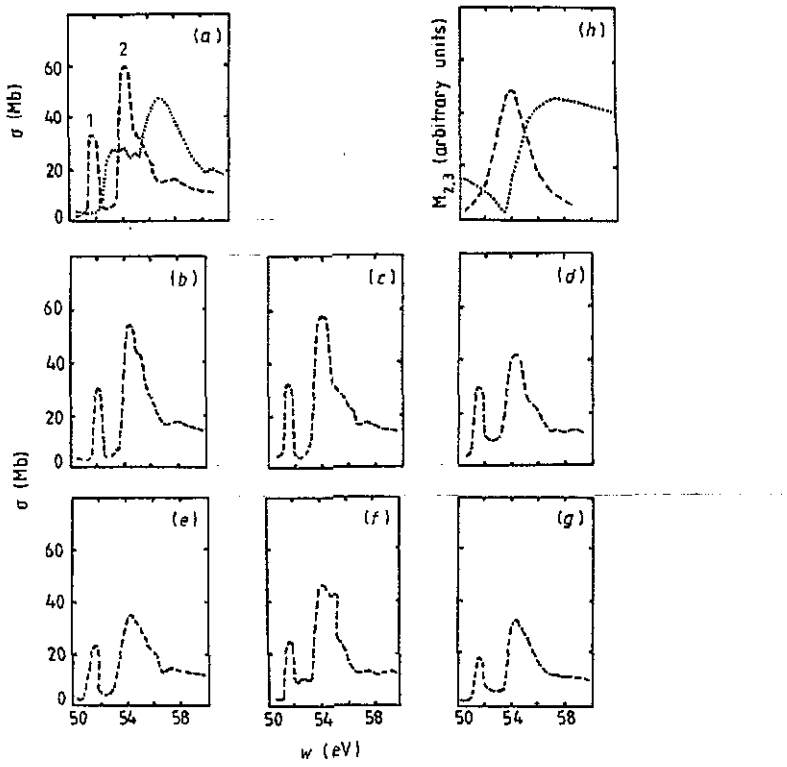

Figure 5. The variation of the giant resonance profile as a function of the size of the iron atomic aggregation: (*a*) the cross section of atomic Fe (broken curve, our calculation; dotted curve, experimental data [28]); (*b*)–(*g*) cross sections of iron clusters containing 9 (*b*), 17 (*c*), 28 (*d*), 66 (*e*), 84 (*f*) and 127 (*g*) atoms; (*h*) $M_{2,3}$ absorption spectrum of bulk iron (broken curve, our calculation; dotted curve, experiment [36]; experimental data are presented in arbitrary units).

of iron clusters are obtained within the local density approach, one can suppose that the cluster spectra are also displaced in the lower energy region.

We have analysed the partial contribution of separate electron excitations to the total photoabsorption cross section as well as the change of the energy position of the resonance with decrease of the induced part of the self-consistent potential (15). (Apparently, when the induced contribution to the self-consistent potential is decreased to zero, the energy of the resonance maximum will approach the energy of the discrete excitation with which the autoionization resonance is connected [35].) Research showed that the giant resonance in the photoabsorption cross section of atomic iron is due to interference between the discrete $3p_\downarrow \rightarrow 3d_\downarrow$ transition and continuum $3d_\uparrow \rightarrow \epsilon p_\uparrow$ (peak 1 in figure 5(*a*)) and $3d_\uparrow \rightarrow \epsilon f_\uparrow$ (peak 2 in figure 5(*a*)) excitations.

The photoabsorption spectra of small iron clusters have been analysed within the framework of the 'atom in jellium' model. The upper part of the potential well for the 'jellium sphere with embedded central Fe atom' system is considerably different from an Fe atomic potential and resembles a spherically symmetric potential well. For this reason, in comparison with an Fe atom, the 'atom in jellium sphere' system can have several discrete d levels. What is more, as distinct from a free Fe atom,

several discrete d states of 'Fe atom in jellium' can be unoccupied. According to selection rules, discrete transitions with p shells on these d levels are possible. The energies of discrete $3p \rightarrow nd$ transitions have close values and lie in the atomic giant resonance range. Since the wavefunctions of the 3p shell and unoccupied d shells overlap considerably, several discrete $3p \rightarrow nd$ transitions can have autoionization character. As a result, the structures of photoabsorption spectra of 'Fe atom in jellium sphere' are more complicated than that of a free Fe atom and depend on the jellium sphere size.

The photoabsorption spectrum of the iron cluster, therefore, consists of 'quasi-atomic' cross sections with various structures. Summation of 'quasi-atomic' spectra and normalization of the sum per atom give the cluster resonance profile, which is more spread than that of a free Fe atom.

Figure 5 illustrates the change of the giant resonance shape of iron with the increase of the atomic aggregation size. As can be seen in the figure, the resonance intensity decreases non-monotonically with the cluster size.

Finally, for comparison, we touch on the absorption of bulk iron in the energy range of 3p-shell excitations. The experimental [36] $M_{2,3}$ absorption spectrum of bulk iron has an asymmetric resonance but, in contrast to the Fe atom, without fine structure (figure 5(*h*)). Our calculations of the $M_{2,3}$ absorption spectrum within the well known one-electron approach (we used the iron electronic band structure obtained by the linear augmented plane-wave method) yield a single symmetric peak at lower energy than the experimental result (figure 5(*h*)). The difference between the experimental and our theoretical results for bulk iron is due to the neglect of many-electron effects, which cause the shift in energy and asymmetric profile of this resonance.

References

[1] Dietz T G, Duncan M A, Powers D E and Smalley R E 1981 *J. Chem. Phys.* **74** 6511–12
[2] Bondybey V E and English J H 1982 *J. Chem. Phys.* **76** 2165–70
[3] Cox D M, Trevor D J, Whetten R L, Rohlfing E A and Kaldor A 1985 *Phys. Rev.* B **32** 7290–8
[4] Whetten R L, Cox D M, Trevor D J and Kaldor A 1985 *Phys. Rev. Lett.* **54** 1494–7
[5] Rohlfing E A, Cox D M and Kaldor A 1983 *Chem. Phys. Lett.* **99** 161–6
[6] Rohlfing E A, Cox D M, Kaldor A and Johnson K H 1984 *J. Chem. Phys.* **81** 3846–51
[7] Martins J L, Car R and Buttet J 1981 *Surf. Sci.* **106** 265–71
[8] Ekardt W 1984 *Phys. Rev.* B **29** 1558–64
[9] Ekardt W 1985 *Phys. Rev.* B **31** 6360–70
[10] Ekardt W 1985 *Solid State Commun.* **54** 83–6
[11] Beck D E 1984 *Solid State Commun.* **49** 381–5
[12] Baladron C and Alonso J A 1988 *Physica* B **154** 73–81
[13] Snider D R and Sorbello R S 1983 *Phys. Rev.* B **28** 5702–10
[14] Manninen M, Nieminen R M and Puska M J 1986 *Phys. Rev.* B **33** 4289–90
[15] Beck D E 1987 *Phys. Rev.* B **35** 7325–33
[16] German M M, Kupershmidt V Ya and Farberovich O V 1989 *Opt. Spektrosk.* **66** 916–19 (in Russian)
[17] German M M, Kupershmidt V Ya, Kurkina L I and Farberovich O V 1990 *Fiz. Tverd. Tela* **32** 1220–2 (in Russian)
[18] Kurkina L I and Farberovich O V 1990 *Phys. Status Solidi* b **160** K37–41
[19] Vosko S H, Wilk L and Nusair M 1980 *Can. J. Phys.* **58** 1200–11
[20] Hermann F and Skillman S 1963 *Atomic Structure Calculations* (Englewood Cliffs, NJ: Prentice-Hall) p 421
[21] Yang C Y, Johnson K H, Salahub D R and Kaspar J 1981 *Phys. Rev.* B **24** 5673–82
[22] Lee K, Callaway J and Dhar S 1984 *Phys. Rev.* B **30** 1724–30

[23] Lee K, Callaway J, Kwong K, Tang R and Ziegler A 1985 *Phys. Rev.* B **31** 1796–803
[24] Tang R and Callaway J 1985 *Phys. Rev. Lett.* A **111** 313–14
[25] Pastor G M, Dorantes-Dávila J and Bennemann K H 1988 *Chem. Phys. Lett.* **148** 459–64
[26] Müller H, Opitz Ch and Romanowski S 1989 *Z. Phys. Chem.* **270** 33–41 (in German)
[27] Whetten R L, Cox D M, Trevor D J and Kaldor A 1985 *Surf. Sci.* **156** 8–35
[28] Meyer M, Prescher Th, von Raven E, Richter M, Schmidt E, Sonntag B and Wetzel H E 1986 *Z. Phys. D.* **2** 347–62
[29] Amusia M Ya 1987 *Atomic Photoeffect* (Moscow: Nauka) p 272 (in Russian)
[30] Zangwill A and Soven P 1980 *Phys. Rev.* A **21** 1561–72
[31] Rajagopal A K 1978 *Phys. Rev.* B **17** 2980–8
[32] Zangwill A and Liberman D A 1984 *Comput. Phys. Commun.* **32** 63–73
[33] Babikov V V 1988 *Phase Function Method in Quantum Mechanics* (Moscow: Nauka) p 256 (in Russian)
[34] Lundqvist S and March N H (ed) 1983 *Theory of the Inhomogeneous Electron Gas* (New York: Plenum) p 395
[35] Nuroh K, Stott M J and Zaremba E 1982 *Phys. Rev. Lett.* **49** 862–6
[36] Nakai S, Nakamori H, Tomita A, Tsutsumi K, Nakamura H and Sugiura C 1974 *Phys. Rev.* B **9** 1870–3